

Variability of dissolved oxygen in the Arabian Sea Oxygen Minimum Zone and its driving mechanisms

Damodar M. Shenoy^{1}, I. Suresh¹, Hema Uskaikar¹, Siby Kurian¹, P. J. Vidya^{1,2},
Gayatri Shirodkar¹, Mangesh U. Gauns¹ and S. W. A. Naqvi^{1,3}*

¹ CSIR-National Institute of Oceanography, Dona Paula, Goa 403004, India.

² National Centre for Polar and Ocean Research, Headland Sada, Goa 403 804, India

³ Council of Scientific and Industrial Research, Anusandhan Bhawan, 2 Rafi Marg, New Delhi, 110001, India

*

Corresponding

author

Abstract:

The Arabian Sea hosts one of the most intense, perennial Oxygen Minimum Zones (OMZ) in the world ocean. Observations along a meridional transect at 68°E extending from 8 to 21°N showed large seasonal as well as interannual changes in the dissolved oxygen and nitrite concentrations. Unlike previous studies that used observations from the periphery of the OMZ, our observations are from its core and also allow us demarcating the southern extent of the OMZ. The southern boundary of the OMZ extended up to ~9°N during the southwest monsoon but was restricted to ~11°N during the northeast monsoon. While previous studies report ventilation from the oxygenated Indian Central Water (ICW) at intermediate depths of the OMZ, none have so far discussed how this ventilation takes place or its variability. Our observations reveal intrusion of the ICW at intermediate depths (200-500 m) into the OMZ up to 16°N, in contrast to 11°N reported in earlier studies. The oxygen variations at the southern boundary of the OMZ are coherent with those in the sea level, associated with the westward propagating Rossby waves radiated off the west coast of India. Besides modulating the oxygen distribution in the surface layer and the upper boundary of the OMZ through upwelling or downwelling, these Rossby waves can potentially influence the oxygen at intermediate depths by controlling the isopycnal mixing of the ICW within the OMZ, leading to variations in oxygen and nitrogen concentrations. Further investigations are needed to better understand the potential influence of these Rossby waves on the OMZ variability and the associated nitrogen cycling.

Keywords: Arabian Sea, Oxygen Minimum Zone, Suboxia, Indian Central Water, Rossby waves

1. Introduction

Oxygen is one of the essential elements for the sustenance of life on Earth. The distribution of dissolved oxygen (DO) in the ocean vary spatially, with zones of low oxygen waters centered around the tropics (Stramma et al., 2008). The northern Indian Ocean (IO), which comprises of the Arabian Sea (AS) and the Bay of Bengal, is one of the major sites in the world oceans with near zero oxygen concentrations at its intermediate depths. The Bay of Bengal is traditionally known to be non-denitrifying (Rao et al., 1994). However, a recent study by Bristow et al. (2016) indicates that it may be at a tipping point and an increase in its productivity due to anthropogenic fluxes may result in a net nitrogen loss. On the other hand, the AS, which houses one of the world's most intense Oxygen Minimum Zones (OMZ; Naqvi et al., 2006), is a strong denitrifying basin that contributes to one-third of the global nitrogen loss to the atmosphere (Bange et al., 2001, 2005; Devol et al. 2006; Naqvi et al. 2006; Ward et al., 2008, 2009; Jayakumar et al., 2009; Paulmeir and Ruiz-Pino, 2009; Jensen et al., 2011; Lam et al., 2011). The AS OMZ (ASOMZ; Figure 1) extends meridionally between 60 and 75°E, zonally between 10 and 25°N (Naqvi, 1991), and vertically between 150 and 1200-m depths (Naqvi, 1991; Naqvi et al., 1994, 1998), with an upward tapering towards the south (Sen Gupta and Naqvi, 1984; Naqvi, 1987; de Souza et al., 1996). One of the intriguing aspects of the ASOMZ is that it is located away from the high productive western boundary upwelling (Somalia and Oman) regions unlike the OMZ's of the Pacific and the Atlantic that are co-located with the highly productive eastern boundary upwelling systems (Naqvi, 1991). Though several theories have been put forth to explain this northeastward shift of the ASOMZ, till date there is no tangible answer to this anomaly (McCreary et al., 2013 and references therein; Acharya and Panigrahi, 2016).

The concentration of DO in the surface waters results from a complex balance between the oxygen produced via primary production, loss via respiration, ventilation through atmospheric exchange and advection by currents. On the other hand, there is no primary production in the subsurface waters, and the DO is generally consumed by heterotrophic processes. In the case of the ASOMZ, the

DO concentration generally reflects the balance between the supply via circulation and the loss via remineralization and respiration, except for its upper boundary. The oxygenated surface waters acts to enhance the DO supply to the upper boundary of the ASOMZ through wind stirring or convective mixing (Morrison et al., 1998). The major supply of oxygen to the northern IO is from the southern hemisphere, where the oxygenated surface waters sink down to intermediate layers and travel northward laterally along the thermohaline gradient and gradually upwell in the AS and in the Bay of Bengal (Wyrski, 1971). Prime among these are the Antarctic waters, which are known to ventilate the deeper layers of the AS thereby limiting the vertical extent of the ASOMZ (Warren 1981). The ASOMZ also receives DO from the following lateral sources, namely the Persian Gulf water (PGW) mass, which intrudes from the northwest at depths of 200 – 300 m (Wyrski, 1971; Shetye et al., 1994; Bower et al., 2000, Prasad et al., 2001) and the Red Sea water (RSW) mass, which is observed at depths between 600 and 800 m (Beal et al., 2000; Sofianos and Johns, 2002; Bower et al., 2005). In addition to these water masses, there is also the Sub-Antarctic mode water (SAMW) that has been reported in the southern sector of the AS (Ivanenkov and Gubin, 1960; Rochford, 1966; Warren, 1981; Sen Gupta and Naqvi, 1984; Naqvi et al., 1993; Ramesh et al 2013). This parcel of low salinity water gets advected from the central IO basin at depths of 200-500 m carrying oxygen with concentrations of 150-220 μM (Ramesh et al., 2013). As it migrates northward, this parcel loses DO but contains a relatively higher concentration of DO when it reaches the southern boundary of the ASOMZ. In an earlier report, Naqvi et al. (1993) had shown that the SAMW dissipates as it enters the southern section ($10 - 11^\circ\text{N}$), losing its oxygen between 200 and 400 m. Using data spanning the two major monsoons, You (1997) described various water masses in the IO and identified the oxygen-rich Indian Central water (ICW) as a major mode for supply of oxygen to the northern IO, but limited its influence to 6°N . On the other hand, Lachkar et al. (2019) describes the ICW as a mixture of the SAMW, Antarctic intermediate waters and the Indonesian intermediate waters, which are advected into the AS via the Somali current. While the above studies refer to the ICW and the SAMW ventilating the ASOMZ, none of them have so far demonstrated how these water masses traverse or mix in the AS.

While the ASOMZ is perennial in nature, previous studies have reported seasonal and interannual variations of DO and nitrite within the OMZ (Naqvi et al., 1990, de Souza et al., 1996, Morrison et al., 1999; Banse et al., 2014). Naqvi et al. (1990) and de Souza et al. (1996) observed severe low oxygen conditions with higher nitrate deficits during the northeast monsoon (NEM). However, Morrison et al., (1999) did not find any major changes in the degree of suboxia in the OMZ within the seasons of 1995. Rixen et al. (2014) found strong seasonal and interannual changes in the ASOMZ from the observations carried out under Joint Global Ocean Flux Study (JGOFS) of 1995 and RV *Meteor* cruise of 2007. These observations, restricted to the north of 15°N, indicated that the ASOMZ retreated eastward during the southwest monsoon (SWM) and expanded westward during the NEM. They attributed these seasonal changes to the variations in the flow of the oxygen-enriched ICW into the OMZ. Banse et al. (2014) used more than four decades of DO measurements from the ASOMZ and reported marked seasonality, with elevated DO levels during the NEM and spring monsoon as compared to the SWM. They also observed a significant decline in the DO levels between 12 and 20°N, but an increasing trend ~21°N from the 4-decade long measurements. Given this scenario and the recent reports on decreasing levels of DO and expansion of OMZs worldwide (Stramma et al., 2008; Keeling et al., 2010; Bopp et al., 2013; Lachkar et al., 2016; Breitburg et al., 2018), the studies on DO variation in the ASOMZ gain further importance. The present paper aims to describe the seasonal and interannual variations of DO and nitrite from the observations carried out along a north-south transect passing through the core of the ASOMZ, unlike earlier studies that used observations from its periphery. We use both physical and chemical measurements to understand how the ICW supplies oxygen to the ASOMZ and possibly influences the nitrogen cycling. In contrast to Rixen et al. (2014), who focused on the western boundary, this study focuses on the southern boundary of the ASOMZ, particularly how the inflow of ICW modulates its southern extent.

Finally, we propose a possible physical control on the inflow of ICW into the ASOMZ. Previous studies (e.g., McCreary et al., 1993; Shankar and Shetye, 1997) suggested that the coastal Kelvin waves along the western Indian continental shelf radiate away Rossby waves. These Rossby waves propagate

westward into the open AS. In recent studies, Suresh et al. (2016; 2018) demonstrated with a linear ocean model that these westward propagating Rossby waves have an important contribution to the sea level variability in the eastern AS (westward up to 65°E) that encompasses our study region. We will discuss the possible role of these Rossby waves in modulating the flow of ICW and thus the DO variability within the ASOMZ.

The paper is organized as follows. Section 2 describes the observations used in this study and the methodology. Section 3 presents the results of this study with a discussion. More specifically, besides describing the seasonal and interannual variations in the DO and nitrite, this section discusses the intrusion of ICW in to the OMZ. Section 4 summarizes the conclusions of this study.

2. Materials and methods

The data presented in this study were collected under two major scientific programs of the Council of Scientific and Industrial Research–National Institute of Oceanography (CSIR-NIO), namely, Sustained Indian ocean Biogeochemistry and Ecosystem Research (SIBER) – India project, and the INDIan Aquatic ecoSystems - Impact of Deoxygenation, Eutrophication and Acidification (INDIAS_IDEA) project using CSIR-NIO's two Research Vessels - RV Sindhu Sankalp (SSK) and RV Sindhu Sadhana (SSD). A transect (Figure 1) along 68°E was sampled during the SWM of 2014 (SSK069; 26th September – 8th October) and 2016 (SSD026; 24th September – 2nd October), and the NEM of 2017 (SSD033; 5 – 14th February). During SSK069, sampling was carried out at alternate stations between 9 and 21°N, whereas during SSD026 and SSD033, sampling was carried out at 1° interval between 8 and 21°N. The temperature and salinity measurements were obtained using a Seabird CTD fitted with a rosette. Nitrite samples were collected in high density plastic bottles after thorough rinsing and were analysed onboard using a Skalar autoanalyser.

DO samples were collected in ground glass stoppered bottles, by overflowing seawater three times the bottle volume to minimise any atmospheric

contamination. The DO samples were fixed and analysed following the Carpenter modification of the Winkler method (Carpenter, 1965). The titration was automated using ODF PC software compiled in LabView, in which the end point is UVC detected photometrically at 365 nm. This methodology gave a precision of 0.1 μM with an accuracy of better than 1%. The detection limit of this automated method (3 μM) is better than the manual titration method (4 μM). We also obtained 1 m DO data from the CTD. While the calibration between CTD DO and automated DO using ODF PC showed a good correlation over the general range up to 210 μM , the lower range calibration was not that good as the CTD DO had a detection limit of only 5 μM . While the high resolution CTD DO data was good enough to delineate the outer boundaries, it was not useful to see the changes within the OMZ (please see supplementary figure). Thus we have used bottle data to generate the DO profiles. In this paper, we have used DO concentration of 5 μM to define the boundary of the suboxic layer (or OMZ), as denitrification sets at DO concentrations of < 5 μM (Morrison et al., 1999; Qasim and Naqvi, 1987, Lam et al., 2011).

Sea level is a good indicator of the internal ocean dynamics. To investigate the possible influence of Rossby waves on our study region, we analyzed the sea level from the AVISO (Archiving, Validation, and Interpretation of Satellite Oceanographic) merged multi-satellite delayed mode weekly product (www.aviso.oceanobs.com/fr/accueil/index.html). We used sea level anomalies (SLA) obtained by removing the long-term linear trend.

3. Results and discussion

3.1. Seasonal and inter-annual variation of Dissolved oxygen and nitrite

Figure 2 shows the oxygen distribution in the upper 1000-m water column along the 68°E meridional transect during the three cruises. The DO concentrations in this layer varied between undetectable levels and 207 μM . In the upper (~50 m) layer, the oxygen concentrations were generally above 180 μM . The oxycline was, in general, around 150-m depth, below which the oxygen concentration was less

than 45 μM . The DO distribution in the top 150-m layer during the NEM was strikingly different compared to that in the SWMs of 2014 and 2016, with clear signatures of oxycline deepening (up to 180 m) between 19 and 21°N, which could probably be resulting from the convective mixing during winter in the northern AS (de Souza et al., 1996). During the SWM of 2014, the southern boundary of the OMZ was observed at ~9°N around 200-m depth. The OMZ then gradually expanded northward to 1000 m at 18°N. In contrast, the shape of the OMZ was different during the SWM of 2016. While the southern boundary was located ~10°N at ~200 m, the tapering shape of the OMZ between 11 and 14°N had changed compared to that in 2014. Trace concentration of DO (~5 μM) was observed to intrude between 400 and 600 m northward of 12°N up to 16°N. A cell of DO concentration (< 5 μM) around 250 m was observed at 17°N in 2016. During the NEM of 2017, the southern limit of the ASOMZ was observed at ~11°N around 200-m depth, but this suboxic layer was thinner compared to 2014 and 2016. As in the case of SWM of 2016 traces of DO (~5 μM) was observed to intrude between 250 and 600 m from 12 to 15°N.

The concentration of DO impacts nitrogen cycling in which nitrate is reduced to nitrite when oxygen level falls below a certain threshold value (Naqvi et al., 1992; Codispoti et al., 2001). The secondary nitrite observed in the ASOMZ is primarily attributed to nitrate reduction and to a lesser degree to ammonium oxidation in the upper OMZ (Lam et al., 2011). The nitrite concentrations (Figure 3), in general, varied between 0.01 and 3.7 μM during the three cruises. The maximum nitrite concentration observed in the OMZ was 3.7 μM in SWM 2014, 3.3 μM in SWM 2016 and 2.7 μM in NEM 2017. In concurrence with the variations of DO (Figure 2), the zone of secondary nitrite maximum (SNM) also expanded towards the north. During the SWM of 2014, it was observed between 100 and 300 m near 11°N, and between 200 and 600 m at 21°N. The shape of the SNM zone during the SWM of 2016 was broadly similar to that in 2014, but with a breakup observed at the southern end, where an isolated cell of nitrite (0.5 - 1 μM) was observed at 11°N. Also, the high nitrite concentration of ~3.7 μM observed at 17°N during 2014 reduced to ~2.1 μM in 2016. Despite these differences in the thickness and the southern extent between 2014 and 2016, the zones of nitrite, in general, were nearly similar, with a single continuous cell (comprising of two or more individual

cells) of SNM extending from the south to the north. On the other hand, the SNM zone during the NEM 2017 was not continuous and was split into several cells with the southernmost cell observed at 200 m (12°N) and the northernmost cell around 18-19°N within 600-700 m. Thus, the nitrite distributions, in conjunction with the DO concentrations, exhibited seasonal and inter-annual variations.

While our measurements agree well with those of de Souza et al. (1996) for the NEM, our observations of clear suboxic conditions during the SWM are strikingly different from their measurements, which indicated higher DO levels. This could be due to fact that their measurements were from 64°E, i.e. from the western periphery of the ASOMZ whereas our observations are from the core of ASOMZ. For similar reasons, our observations are in a stark contrast to Morrison et al. (1999), who used observations away from the core of the ASOMZ and Naqvi et al. (1990), whose observations were confined to the north-eastern part of the AS between 15 and 22°N. Our observations indicate contrasting features compared to those of Rixen et al. (2014), whose observations were confined to the western AS and north of 15°N. Our results, however agree with Banse et al. (2014), who processed 4 decades of DO data from the ASOMZ and reported higher oxygen concentrations between 200 and 500 m depth during the NEM than the SWM. In the following section, we focus on how the supply via ICW modulates the oxygen variability within the OMZ, especially its southern boundary that is hitherto not well addressed in the previous studies.

3.2. Supply of oxygen to the ASOMZ

While the ASOMZ was well defined during the SWM of 2014, the presence of higher DO concentration during the SWM of 2016 and NEM of 2017 suggests possible oxygen supply by a water mass to the ASOMZ. Figure 2 indicates such a parcel of water at the southern end of the transect (8 – 10°N) supplying oxygen to the OMZ at depths between 200 and 500 m. This parcel of water was characterised by a low salinity of 35.25 psu and a high DO of ~50 μM (Figures 2 and 4). Figure 4 further shows high variability in the distribution of this low saline water along the track during the 3 cruises. Moreover, this figure demonstrates intrusion of the above low saline water up to 16°N and its interaction with the PGW

during the SWM of 2016 and NEM of 2017. During the SWM of 2016 at 16°N below 200 m, a parcel of PGW (as seen from high salinity of 35.75 psu) is surrounded by a parcel of low saline water (<35.75; Figure 4) with higher traces of DO (Figure 2). Similarly, during the NEM of 2017, a parcel of low saline water (35.25) is observed at 16°N (Figure 4). This low saline high DO water mass was first identified by Ivanenkov and Gubin (1960), who called it the subtropical subsurface water. Later, Rochford (1966) described the same water mass as subtropical oxygen maximum water due to its high oxygen content. They also observed that a single branch of this northward moving water mass around 300 m gets separated in to at least three branches of sigma t values of 25.9, 26.5 and 26.8 in the depth range of 200 - 500 m, which is similar to the sigma t values in our case for the low saline high oxygen water observed at the similar depth range during the SWM of 2016 and NEM of 2017 (Figure 5). Following Lachkar et al. (2019), we will refer to a mixture of the above water mass, Antarctic Intermediate water and the Indonesian Intermediate water as ICW.

The influence of the oxygenated ICW water mass on nitrite concentrations is shown in Figure 3. While nitrite concentration during SWM 2016 is reduced compared to that in 2014, the SNM build up almost collapsed in NEM 2017 (only a few isolated cells of nitrite in NEM 2017, shown in Figure 3). Thus the ICW intrudes up to 16°N in to the ASOMZ, and influences the DO and nitrite distributions.

To further illustrate the intrusion of ICW into the OMZ, we plotted the TS profiles for the 3 cruises, with DO concentration overlaid (Figure 5). This figure shows the maximum number of samples with high DO (~50 µM, blue dots; within the temperature range 7 - 13°C, salinity ~35.25 psu and density 25.9 - 26.8) in the depth range of 200 -500 m during the NEM 2017, followed by the SWM 2016 and the least during the SWM 2014. In the next section, we will discuss a physical control on the movement of ICW into the ASOMZ.

3.3. Possible influence of Rossby waves on the ASOMZ

As discussed in the introduction, our observational transect lies in the eastern AS, which is strongly influenced by the westward propagating Rossby waves radiated off the west coast of India. Recent observational and modeling based studies (Prakash et al., 2013; Parvathi et al., 2017) demonstrated that the sea level and hence the thermocline depth changes induce variations in the oxycline depths, which in turn can potentially influence the DO concentration in the upper layer. This motivated us to investigate the effect of those westward propagating Rossby waves on the DO distribution in the surface layer and upper boundary of the ASOMZ.

Figure 6 illustrates the westward propagation of Rossby waves from the west coast of India along 10°N. Positive SLAs indicate downwelling signals, which deepen the oxygenated surface layer, thereby oxygenating the upper boundary of the OMZ. Negative SLAs indicate upwelling signals, which shoal the oxycline depth, thereby inhibiting oxygenation of the upper boundary of the OMZ. At 10°N (Figure 6), the NEM 2017 (5 – 14th February) is characterized by downwelling signals, favoring higher DO concentration compared to that during the SWM (26th September – 8th October 2014 and 24th September – 2nd October 2016), which is characterized by upwelling signals. This explains the difference in the southern extent of ASOMZ between NEM and SWM.

Besides modulating the oxygen distribution in the surface layer and the upper boundary of the OMZ through upwelling or downwelling (through oxycline depth variations), the above Rossby waves can potentially influence the oxygen at intermediate depths by controlling the isopycnal mixing of the ICW within the OMZ as follows. While upwelling suppresses the vertical supply of oxygen from the oxygenated surface layer to the OMZ, it can favor intrusion of the oxygenated ICW to the OMZ. Similarly, downwelling increases the supply of oxygen from the oxygenated surface layer to the OMZ, but suppresses intrusion of the ICW to the OMZ. Banse et al. (2014) indicated that the supply of oxygen to the OMZ at 200 - 500 m depths mainly occur along isopycnals. This implies that the baroclinic Rossby waves can have a strong influence on the supply of oxygen from water masses along isopycnals at deeper levels (the first baroclinic Rossby wave typically extend beyond 500 m depth).

Figure 7 displays the observed sea level along the transect. It shows that during the SWM of 2014, the section of transect from $\sim 11.5^{\circ}\text{N}$ to 17°N was experiencing downwelling conditions (positive sea level), whereas during the SWM of 2016 the section of transect from 8°N to 17°N was experiencing upwelling conditions (negative sea level). These are clearly shown in the temperature sections (Figure 8), which indicates more lower temperature isotherms in the 100 - 200 m depth range (black dotted box) during the SWM of 2016 in comparison to the SWM of 2014. The downwelling during the SWM of 2014 restricts the northward propagation of the ICW, thereby sustaining the ASOMZ suboxic conditions. On the other hand, the upwelling during SWM of 2016 favors the northward propagation of ICW, supplying oxygen to the OMZ.

3.4. Impact of ICW on ASOMZ

The impact of ICW on ASOMZ is evident in Figures 2 and 3, which show a well-defined OMZ extending down to 9°N during the SWM 2014, with a thicker nitrite bearing zone, whereas the OMZ and hence the nitrite zone are thinner during the SWM 2016. During the NEM of 2017, a large part of transect experienced upwelling conditions (Figures 7 and 8) and the northernmost section (blue box in Figure 8) experienced winter convective mixing as seen from the low-temperature isotherms. This had a dual impact on oxygen supply: in the southern section (south of 14°N), the oxygen supply is through ICW and in the northern section (north of 14°N), the oxygen supply is via convective winter mixing. Overall, there was a higher supply of oxygen to the OMZ during NEM 2017 (Figure 2), which led to decimating the OMZ as indicated by the complete fracture in the nitrite bearing zone and also deepening of the nitrite bearing zone down to 600 – 800 m (Figure 3).

4. Conclusion:

In the present study, a north-south transect extending from 8 to 21°N along 68°E was sampled for biogeochemical parameters (dissolved oxygen and nitrite concentrations) during the SWMs of 2014 and 2016 and the NEM of 2017.

Considerable seasonal as well as inter-annual variability was observed in the dissolved oxygen and nitrite distribution. While the OMZ was well defined during the SWM of 2014 with the southern boundary around 9°N, it was observed ~10°N during the SWM of 2016 with a resultant loss in the thickness of nitrite bearing zone. In comparison, the southern boundary was observed ~11°N during the NEM of 2017 with a maximum supply of oxygen to the ASOMZ and a complete fracture of the nitrite bearing zone. The ICW was found to be the primary source of oxygen to the OMZ at depths between 200 and 500 m. Its influence was found up to 16°N. We propose that the westward propagating Rossby waves from the west coast of India strongly influence the ASOMZ by modulating the flow of ICW into the OMZ. Our present set of observations however do not allow in-depth analyses of the underlying physical processes, which may further require a dedicated modeling approach.

Acknowledgment:

The authors thank the Director, CSIR-NIO, for infrastructural facilities and support. The authors are grateful to H. Dalvi, Richita Naik, N. Mohan, S Manjrekar, A. Patil, M. Kerkar, M. Naik, B. Patole and K. Kumar for providing the necessary technical support during the cruises. This study was carried out as a part of the INDIAS_IDEA project (PSC0108) funded by the Council of Scientific and Industrial Research and the SIBER-INDIA project (GAP2425) funded by the Ministry of Earth Sciences. This is NIO's Contribution no.

References:

1. Acharya, S.S. and Panigrahi, M.K., 2016. Eastward shift and maintenance of Arabian Sea oxygen minimum zone: Understanding the paradox. *Deep Sea. Res. I*, 115, 240-252.
2. Bange, H.W., Andreae, M.O., Lal, S., Law, C.S., Naqvi, S.W.A., Patra, P.K., Rixen, T. Upstill-Goddard, R.C., 2001. Nitrous oxide emissions from the Arabian Sea: A synthesis. *Atmos. Chem. Phys.*, 1, 61-71.
3. Bange, H.W., Naqvi, S.W.A and Codispoti, L.A., 2005. The nitrogen cycle in the Arabian Sea. *Prog. In Oceanogr.*, 65, 145-158.
4. Banse, K., Naqvi, S.W.A., Narvekar, P.V., Postel, J.R. and Jayakumar, D. A., 2014. Oxygen minimum zone of the open Arabian Sea: variability of oxygen and nitrite from daily to decadal timescales. *Biogeosciences*, 11, 2237–2261. Doi:10.5194/bg-11-2237-2014.
5. Beal, L. M., Field, A. and Gordon, A. L., 2000. Spreading of Red Sea overflow waters in the Indian Ocean, *J. Geophys. Res.*, 105(C4), 8549–8564.
6. Bopp, L., Resplandy, L., Orr, J. C., Doney, S. C., Dunne, J. P., Gehlen, M., Halloran, P., Heinze, C., Ilyina, T., Séférian, R., Tjiputra, J. and Vichi, M., 2013. Multiple stressors of ocean ecosystems in the 21st century: projections with CMIP5 models. *Biogeosciences*, 10, 6225-6245.
7. Bower, A. S., Hunt, H. D. and Price, J. F., 2000. Character and dynamics of the Red Sea and Persian Gulf outflows, *J. Geophys. Res.*, 105(C3), 6387–6414.
8. Bower, A. S., Johns, W. E., Fratantoni, D. M. and Peters, H., 2005. Equilibration and circulation of Red Sea Outflow Water in the Western Gulf of Aden, *J. Phys. Oceanogr.*, 35, 1963–1985.
9. Breitburg, D., Levin, L.A., Oschlies, A., Grégoire, M., Chavez, F. P., Conley, D.J. Garçon, V., Gilbert, D., Gutiérrez, D., Isensee, K., Jacinto, G.S., Limburg, K.E., Montes, I., Naqvi, S.W.A., Pitcher, G.C., Rabalais, N.N., Roman, M.R., Rose, K.A., Seibel, B.A., Telszewski, M., Yasuhara, M. and Zhang, J., 2018. Declining oxygen in the global ocean and coastal waters. *Science*. 359 (46), DOI: 10.1126/science.aam7240.
10. Bristow, L. A., Callbeck, C. M., Larsen, L., Altabet, M.A., Dekaezemacker, J. Forth, M., Gauns, M., Glud, R. N., Kuypers, M. M. M. Lavik, G., Milucka, J., Naqvi, S.W. A. Pratihary, A., Revsbech, N. P., Thamdrup, B., Treusch, A. H. and Canfield, D. E. 2016. N₂ production rates limited by nitrite availability in the Bay of Bengal oxygen minimum zone, *Nat. Geosc.*, DOI: 10.1038/NNGEO2847.

11. Carpenter, J. H., "The Chesapeake Bay Institute technique for the Winkler dissolved oxygen method," *Limnology and Oceanography*, 10, pp. 141-143 (1965)
12. Codispoti, L.A., Brandes, J.A., Christensen, J.P., Devol, A.H., Naqvi, S.W.A., Pearl, H.W. and Yoshinari, T. 2001. The oceanic fixed nitrogen oxide budgets: Moving targets as we enter the anthropocene? *Sci. Mar*, 65 (suppl 2), 85-105
13. de Souza, S.N., Kumar, M.D., Sardesai, S., Sarma, V.V.S.S. and Shrodkar, P.V., 1996. Seasonal variability in oxygen and nutrients in the central and eastern Arabian Sea. *Curr. Sci.*, 71 (11), 847-851.
14. Devol, A.H., Uhlenhopp, A.G., Naqvi, S.W.A., Brandes, J.A., Jayakumar, D.A., Naik, H., Gaurin, S., Codispoti, L.A. and Yoshinari, T., 2006. Denitrification rates and excess nitrogen gas concentrations in the Arabian Sea oxygen deficient zone. *Deep Sea. Res. I*, 53, 1533-1547.
15. Ivanenkov, V.N. and Gubin, F.A., 1960. Water masses and hydro-chemistry of the western and southern parts of the Indian Ocean. *Transactions of the Marine Hydrophysical Institute, Academy of Sciences of the USSR*, 22, 27-99, A.G.U.
16. Jayakumar, A., Mullan, G. D. O., Naqvi, S. W. A. and Ward, B. B., 2009. Denitrifying Bacterial Community Composition Changes Associated with Stages of Denitrification in Oxygen Minimum Zones. *Microb. Ecol.*, 58, 350-362. DOI 10.1007/s00248-009-9487-y
17. Jensen, M. M, Lam, P., Revsbech, N.P., Nagel, B., Gaye, B., Jetten, M.S.M. and Kuypers, M.M.M., 2011. Intensive nitrogen loss over the Omani Shelf due to anammox coupled with dissimilatory nitrite reduction to ammonium. *The ISME Journal*, 5, 1660-1670.
18. Keeling, R.E., Kortzinger, A. and Gruber, N., 2010. Ocean deoxygenation in a warming world. *Ann. Rev. Mar. Sci.*, 2, 199-229.
19. Lachkar, Z., Smith, S., Lévy, M. and Pauluis, O., 2016. Eddies reduce denitrification and compress habitats in the Arabian Sea. *Geophys. Res. Lett.*, 43, doi:10.1002/2016GL069876
20. Lachkar, Z., Levy, M. and Smith, K.S., 2019. Strong Intensification of the Arabian Sea Oxygen Minimum Zone in response to Arabian Gulf Warming. *Geophys. Res. Lett.*, 46, 5420-5429.
21. Lam P., Jensen¹, M. M. Kock, A., Lettmann, K. A., Plancherel, Y., Lavik, G., Bange, H. W. and Kuypers, M. M. M., 2011. Origin and fate of the secondary nitrite maximum in the Arabian Sea. *Biogeosciences*, 8, 1656-1577.

22. McCreary, J. P., Jr., P. K. Kundu, and R. L. Molinari (1993), A numerical investigation of dynamics, thermodynamics and mixed-layer processes in the Indian Ocean, *Prog. Oceanogr.*, 31(3), 181–244, doi:10.1016/0079-6611(93)90002-U.
23. McCreary, J. P., Yu, Z., Hood, R. R., Vinaychandran, P., Furue, R., Ishida, A. and Richards. K. J., 2013. Dynamics of the Indian-Ocean oxygen minimum zones, *Prog. Oceanogr.*, 112, 15–37.
24. Morrison, J. M., Codispoti, L. A., Gaurin, S., Jones, B., Manghnani, V., and Zheng, Z. 1998. Seasonal variation of hydrographic and nutrient fields during the US JGOFS Arabian Sea Process Study. *Deep-Sea Research II*, 45, 2053–2101.
25. Morrison, J. M., Codispoti, L. A., Smith, S. L., Wishner, K., Flagg, C., Gardner, W. D., et al. 1999. The oxygen minimum zone in the Arabian Sea during 1995. *Deep-Sea Research II*, 46, 1903–1931.
26. Naqvi, S.W.A., 1987. Some aspects of the oxygen-deficient conditions and denitrification in the Arabian Sea. *J. of Mar. Res.* 45, 1049-1072.
27. Naqvi, S.W.A., Noronha, R.J., Somasundar, K. and Sen Gupta, R. 1990. Seasonal changes in the denitrification regime of the Arabian Sea. *Deep-Sea Res.*, 37, 593-611.
28. Naqvi, S.W.A., 1991. Geographical extent of denitrification in the Arabian Sea in relation to some physical processes. *Oceanol. Acta.*, 14, 281-290.
29. Naqvi, S.W.A., Noronha, R.J., Shailaja, M.S., Somasundar, K. and SenGupta, 1992. Some aspects of the nitrogen cycling in the Arabian Sea. *In: Oceanography of the Indian Ocean*. Eds. Desai, B.N., 285-311.
30. Naqvi, S.W.A., Kumar, M.D., Narvekar, P.V., de Souza, S.N., George, M.D. and D'Silva, C.D., 1993. An intermediate nepheloid layer associated with high microbial metabolic rates and deintrification in the northwest Indian Ocean. *J. Geophys. Res.*, 98 (C9), 16469-16479.
31. Naqvi, S.W.A., 1994. Denitrification processes in the Arabian Sea. *Proc. Indian Acad. Sci. (Earth Planet Sci.)*, 103 (2), 279-300.
32. Naqvi, S.W.A., Yoshinari, T., Jayakumar, D. A. Altabet, M. A. Narvekar, P. V. Devol, A. H., Brandes, J. A. and Codispoti, L. A., 1998. Budgetary and biogeochemical implications of N₂O isotope signatures in the Arabian Sea. *Nature*, 394, 462-464.
33. Naqvi, S.W.A., Naik, H., Pratihary, A.K., DeSouza, W., Narvekar, P.V., Jayakumar, D.A., Devol, A.H., Yoshinari, T., Saino, T. 2006. Coastal versus open-ocean denitrification in the Arabian Sea. *Biogeosciences*, 3(3); 2006, 621-633.

34. Parvathi, V., Suresh, I., Lengaigne, M., Ethe, C., Vialard, J., Levy, M., Neetu, S., Aumont, O., Resplandy, L., Naik, H., & Naqvi, W. (2017). Positive Indian Ocean Dipole events prevent anoxia along the west coast of India. *Biogeosciences*, 14 (6), 1541-1559, <https://doi.org/10.5194/bg-14-1541-2017>.
35. Paulmeir, A and Ruiz-Pino, D. 2009. Oxygen minimum zones (OMZs) in the modern ocean. *Prog. In Oceanogr.* 80, 113-128.
36. Prakash, S., Prakash, P, and Ravichandran, M. 2013. Can oxycline depth be estimated using sea level anomaly (SLA) in the northern Indian Ocean?, *Remote Sensing Letters*, 4:11, 1097-1106, DOI: 10.1080/2150704X.2013.842284
37. Prasad, T.G., Ikeda, M., PrasannaKumar, S., 2001. Seasonal spreading of the Persian Gulf water mass in the Arabian Sea. *J. Geophys. Res.*, 106 (C8), 17059-17071
38. Qasim, S.Z. and Naqvi, S.W.A., 1987. Marine nitrogen cycling- Some recent observations in the northwestern Indian Ocean. *Advances in Aquatic Biology and Fisheries*. Prof. N. Balakrishnan Nair Felicitation Volume. eds. by: Natarajan, P.; Suryanarayanan, H.; Azis, P.K.A. Univ. of Kerala; Trivandrum; India; 1987; 13-21
39. Ramesh, S., Ramadass, G.A., Ravichandran, M. and Atmanand, M.A., 2013. Dissolved oxygen as a tracer for intermediate water mixing characteristics in the Indian Ocean. *Curr. Sci.*, 105 (12), 1724-1729.
40. Rao, C.K., Naqvi, S.W.A. Kumar, M.D., Varaprasad, S.J.D., Jayakumar, D.A., George, M.D. and Singbal, S.Y.S., 1994. Hydrochemistry of the Bay of Bengal: possible reasons for a different water-column cycling of carbon and nitrogen from the Arabian Sea. *Mar. Chem.*, 47, 279-290.
41. Rochford, D.J., 1966. Source regions of oxygen maxima in intermediate depths of the Arabian Sea. *Australian Journal of Marine and Freshwater Research*, 17, 1-30.
42. Rixen, T., Baum, A. Gaye, B. and Nagel, B. 2014. Seasonal and interannual variations in the nitrogen cycle in the Arabian Sea. *Biogeosciences*, 11, 5733 – 5747.
43. Sen Gupta, R. and Naqvi, S.W.A., 1984. Chemical oceanography of the Indian Ocean, north of the equator. *Deep-Sea Res.*, 31, 671-706.
44. Shankar, D., and S. R. Shetye (1997), On the dynamics of the Lakshadweep high and low in the southeastern Arabian Sea, *J. Geophys. Res.*, 102(C6), 12,551–12,562, doi:10.1029/97JC00465.

45. Shetye, S.R., Gouveia, A.D., Shenoi, S.S.C., 1994. Circulation and water masses of the Arabian Sea. *Biochemistry of the Arabian Sea: Present information and gaps.* ed. by: Lal, D. (Proc. Indian Acad. Sci. (Earth Planet. Sci.)). Indian Acad. of Sci., Bangalore, India: 103 (2), 1994, 107-123.
46. Sofianos, S. and Johns, W.E., 2002. Water mass formation, overturning circulation, and the exchange of the Red Sea with the adjacent basins. *The Red Sea.* Rasul, N.M.A. and Stewart, I.C.F. (eds.), Springer Earth System Sciences, DOI 10.1007/978-3-662-45201-1_20.
47. Stramma, L., Johnson, G.C., Sprintall, J. and Mohrholz. V., 2008. Expanding Oxygen-Minimum Zones in the Tropical Oceans, *Science*, 320, 655-658.
48. Suresh, I., J. Vialard, T. Izumo, M. Lengaigne, W. Han, J. McCreary, and P. M. Muraleedharan, 2016. Dominant role of winds near Sri Lanka in driving seasonal sea level variations along the west coast of India, *Geophys. Res. Lett.*, 43, 7028–7035, doi: 10.1002/2016GL069976.
49. Suresh, I., Vialard, J., Lengaigne, M., Izumo, T., Parvathi, V., & Muraleedharan, P. M., 2018. Sea level interannual variability along the west coast of India, *Geophys. Res. Lett.*, 45, 12440-12448.
50. Ward, B.B., Tuit, C.B., Jayakumar, D.A., Rich, J.J., Moffett, J., Naqvi, S.W.A., 2008. Organic carbon, and not copper, controls denitrification in oxygen minimum zones of the ocean. *Deep-Sea Res. I*, 55, 1672-1683. Doi:10.1016/j.dsr.2008.07.005
51. Ward, B.B., Devol, A. H. Rich, J. J., Chang, B. X., Bulow, S. E., Naik, H., Pratihary, A. and Jayakumar, D.A. 2009. Denitrification as the dominant nitrogen loss process in the Arabian Sea. *Nature*, 461, 78-82. Doi:10.1038/nature08276
52. Warren, B.A., 1981. Transindian hydrographic section at Lat. 18°S. Property distribution and circulation in the South Indian Ocean. *Deep-Sea Res.*, 28, 759-788.
53. Wyrtki, K., 1971. *Oceanographic Atlas of the International Indian Ocean Expedition.* National Science Foundation, Washington, D.C., 531 pp.
54. You, Y. 1997. Seasonal variations of thermocline circulation and ventilation in the Indian Ocean. *J. of Geophys. Res.*, 102, C5, 10391-10422.

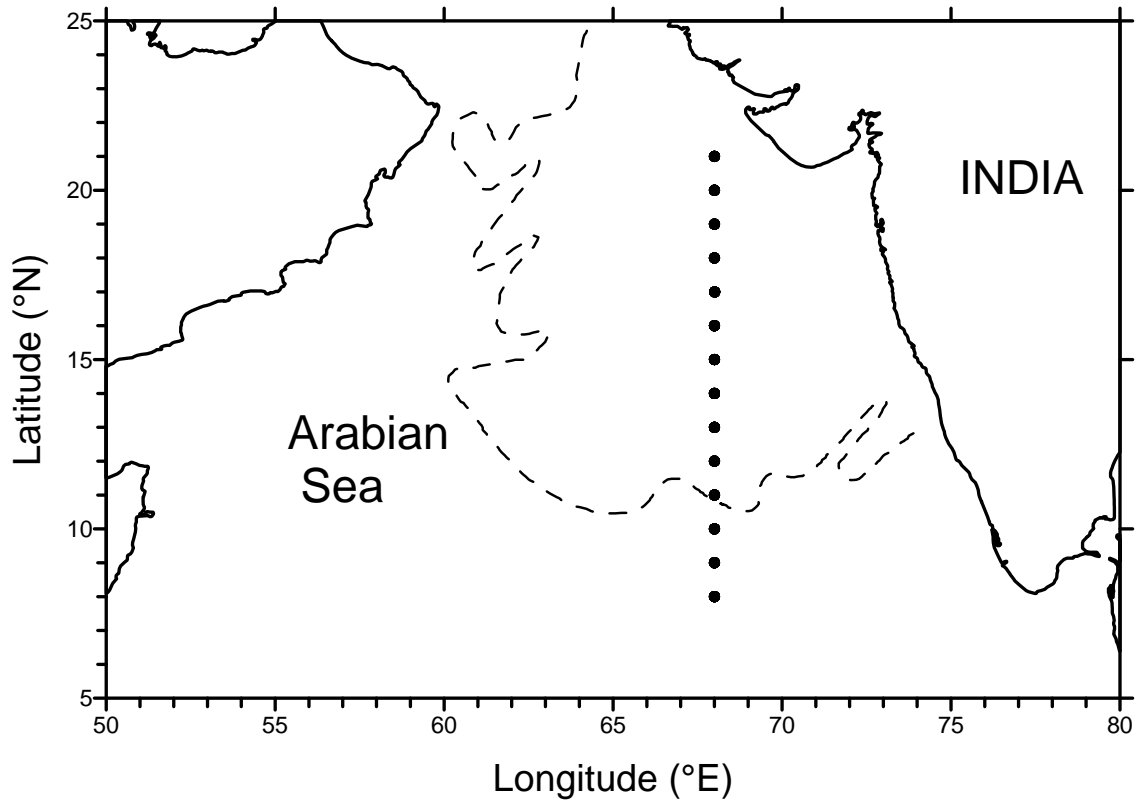


Figure 1. Station locations in the Arabian Sea extending from 8° to 21°N along 68°E. The dashed line shows the contour for 0.2 μM of nitrite from Naqvi (1991) and is the generally accepted boundary of the ASOMZ.

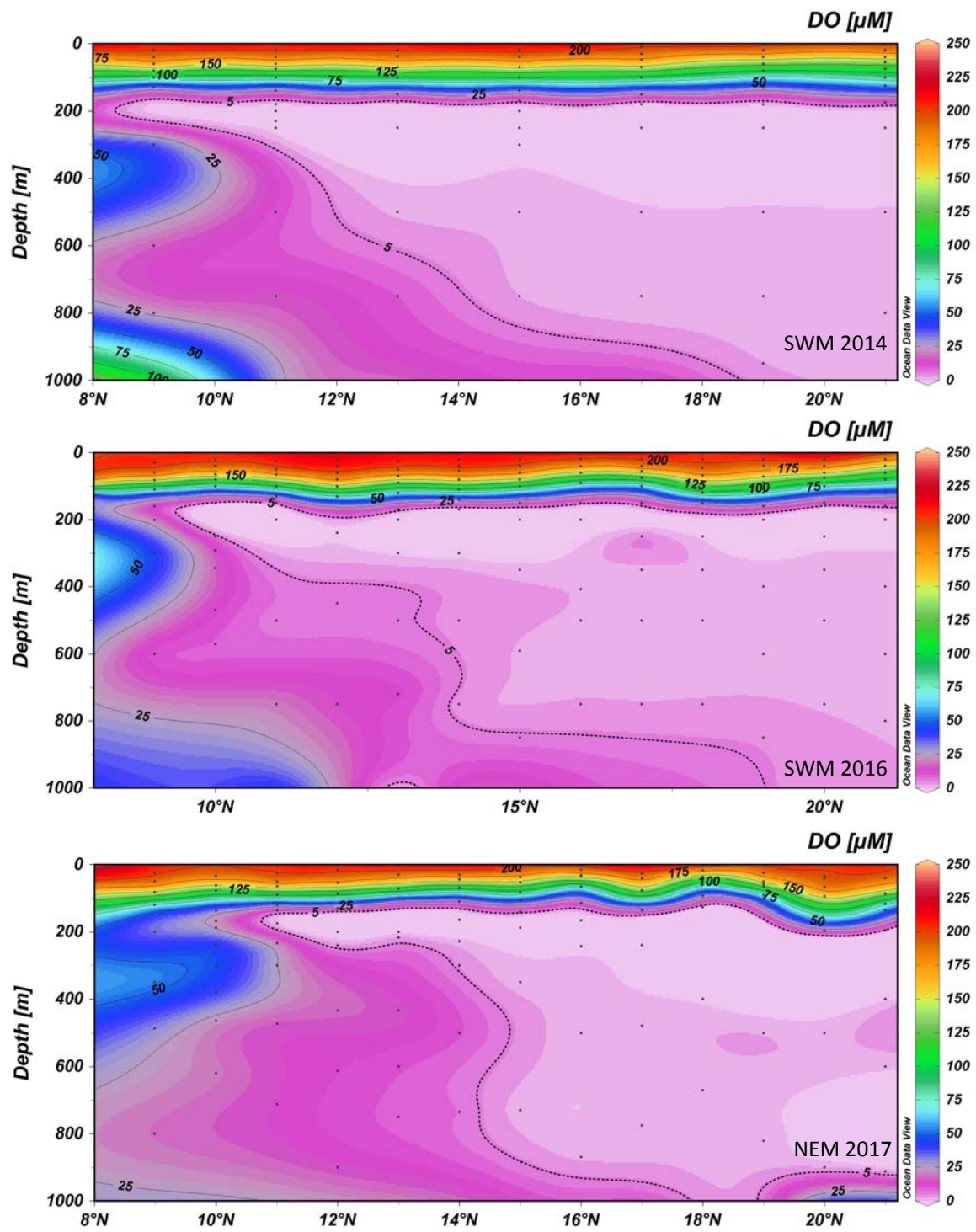


Figure 2. Variation of dissolved oxygen between 8 and 21°N along 68°E longitude during the SWM of 2014 and 2016, and during the NEM of 2017.

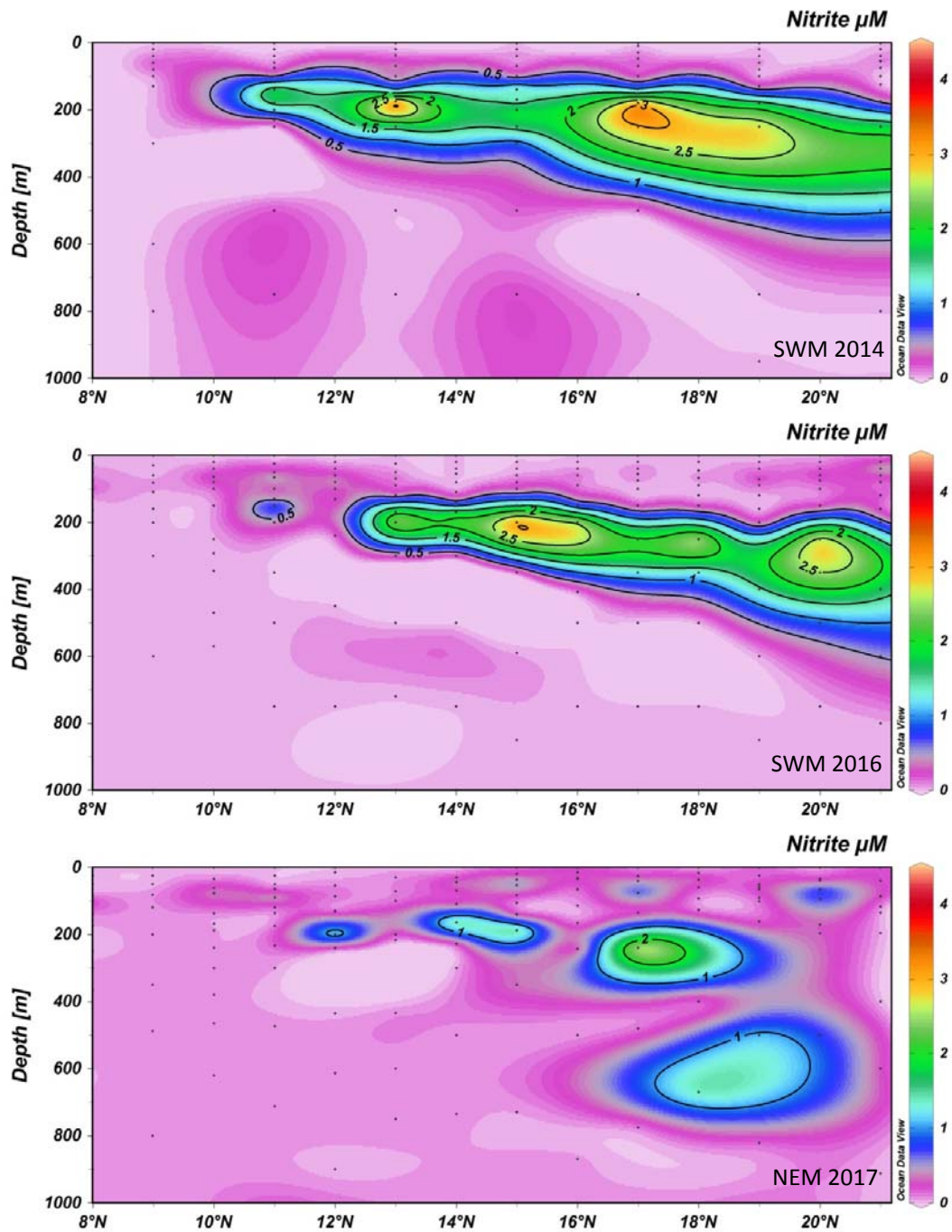


Figure 3. Variation of nitrite between 8 and 21°N along 68°E longitude during the SWM of 2014 and 2016, and during the NEM of 2017.

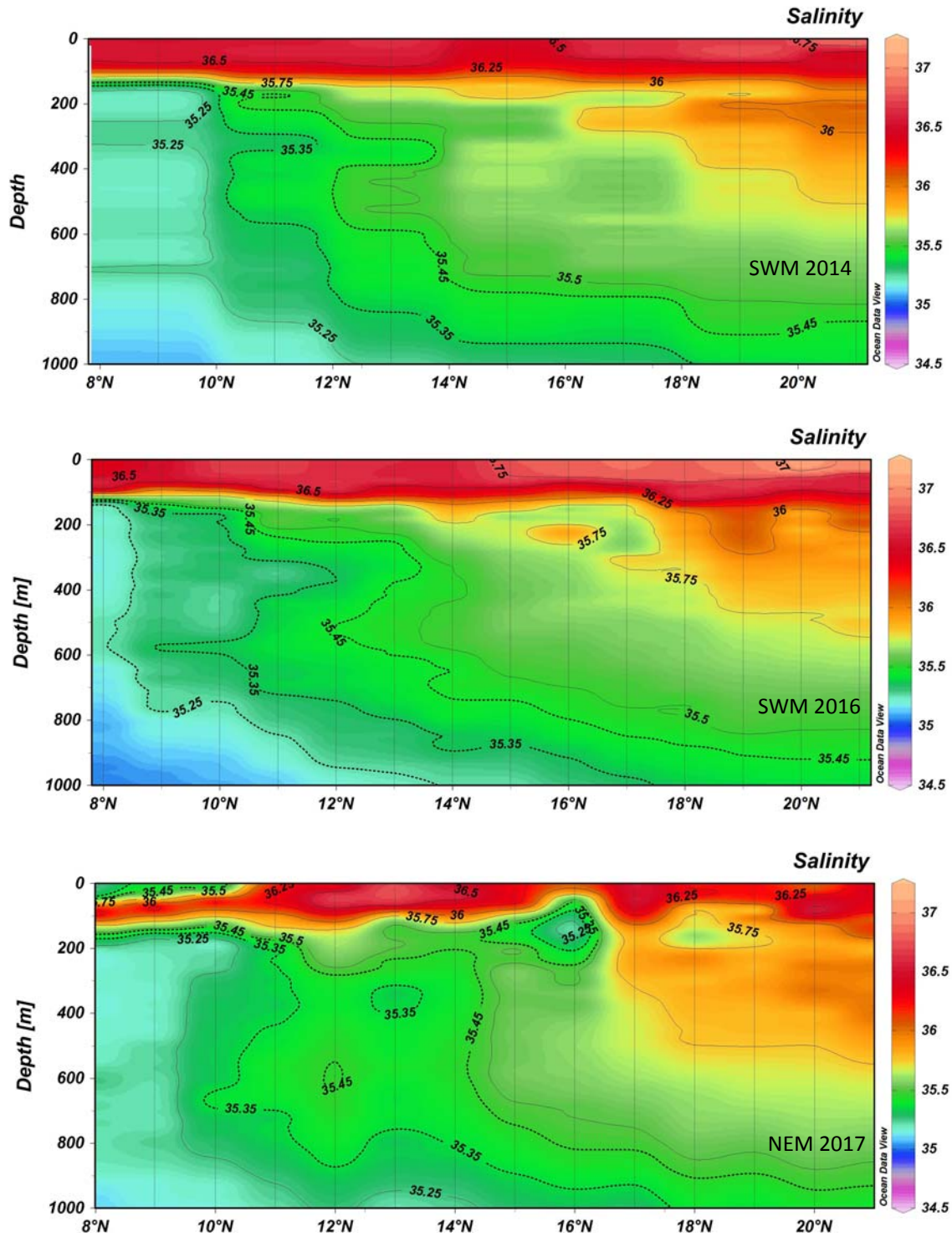


Figure 4. Variation of salinity (psu) between 8 and 21°N along 68°E longitude during the SWM of 2014 and 2016, and during the NEM of 2017.

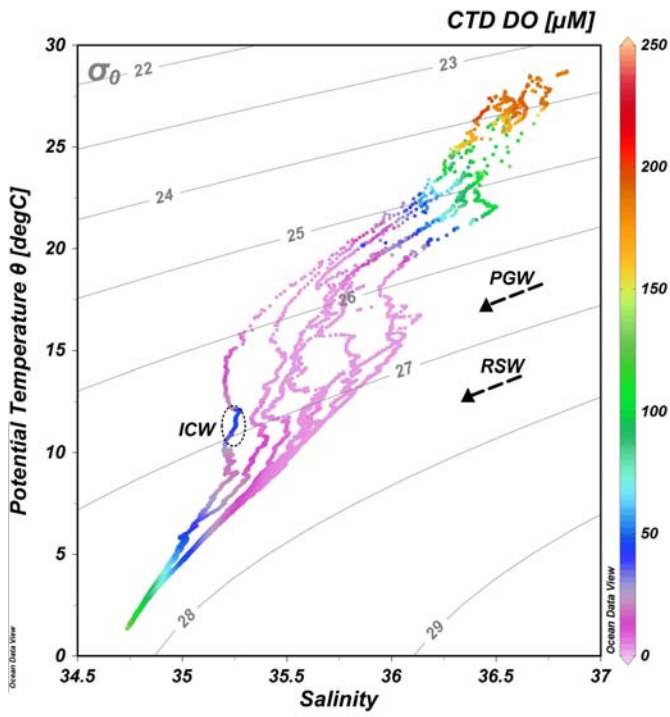
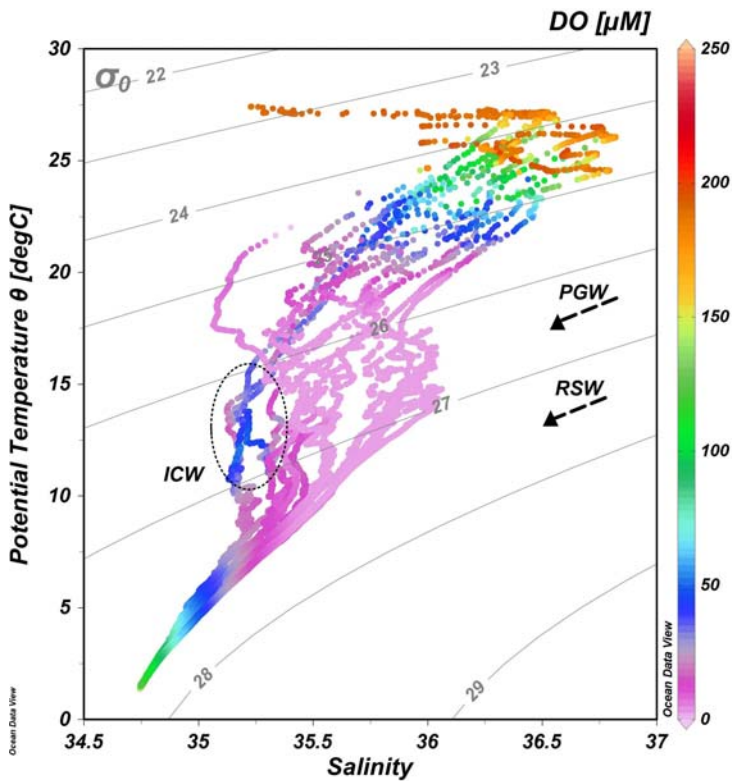
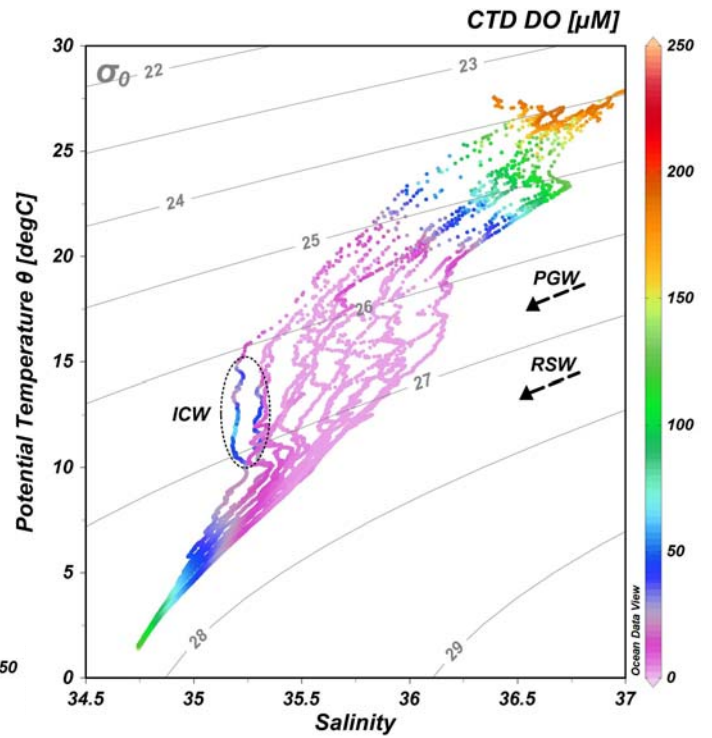


Figure 5. T-S diagram for the SWM of 2014 and 2016, and for the NEM of 2017. The colour of the dots shows the DO concentration. The bluish dots in the ellipse are the Indian Central waters as defined by the salinity of ~ 35.25 and temperature between 11° and 17°C . Note the higher number of bluish dots in the ellipse during the NEM of 2017 and the SWM of 2016 in comparison to the SWM of 2014.



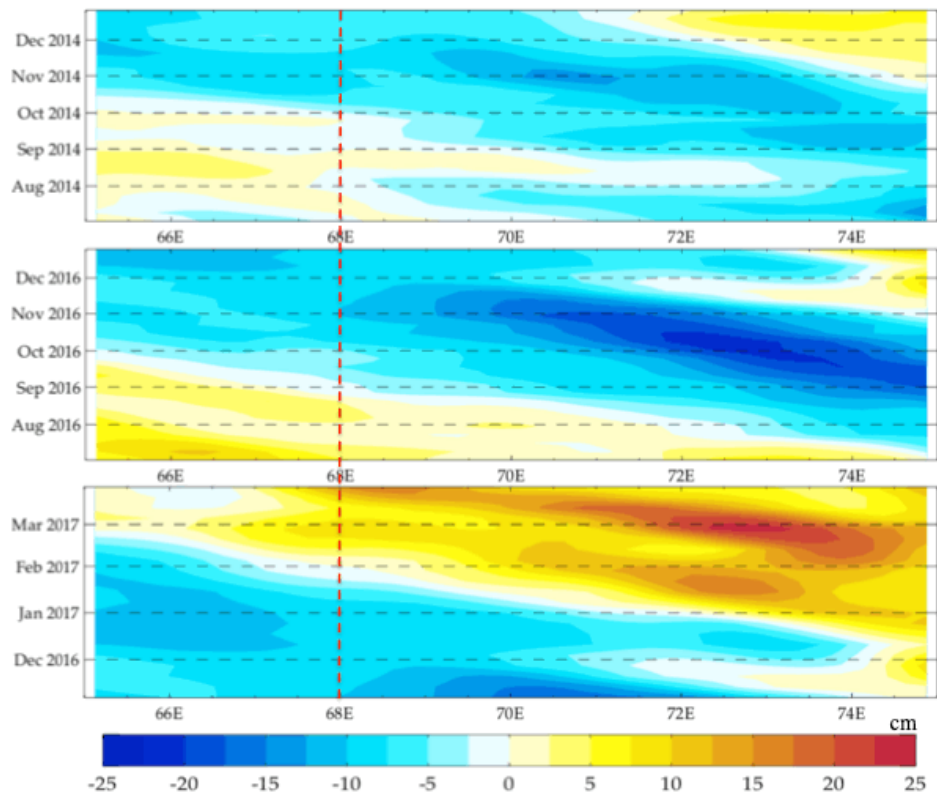


Figure 6. The longitude-time plot of the observed sea level (in cm) at 10°N during the SWM of 2014 and 2016 and, the NEM of 2017. The 68°E , where our observational transect is located, is marked with a dashed red line.

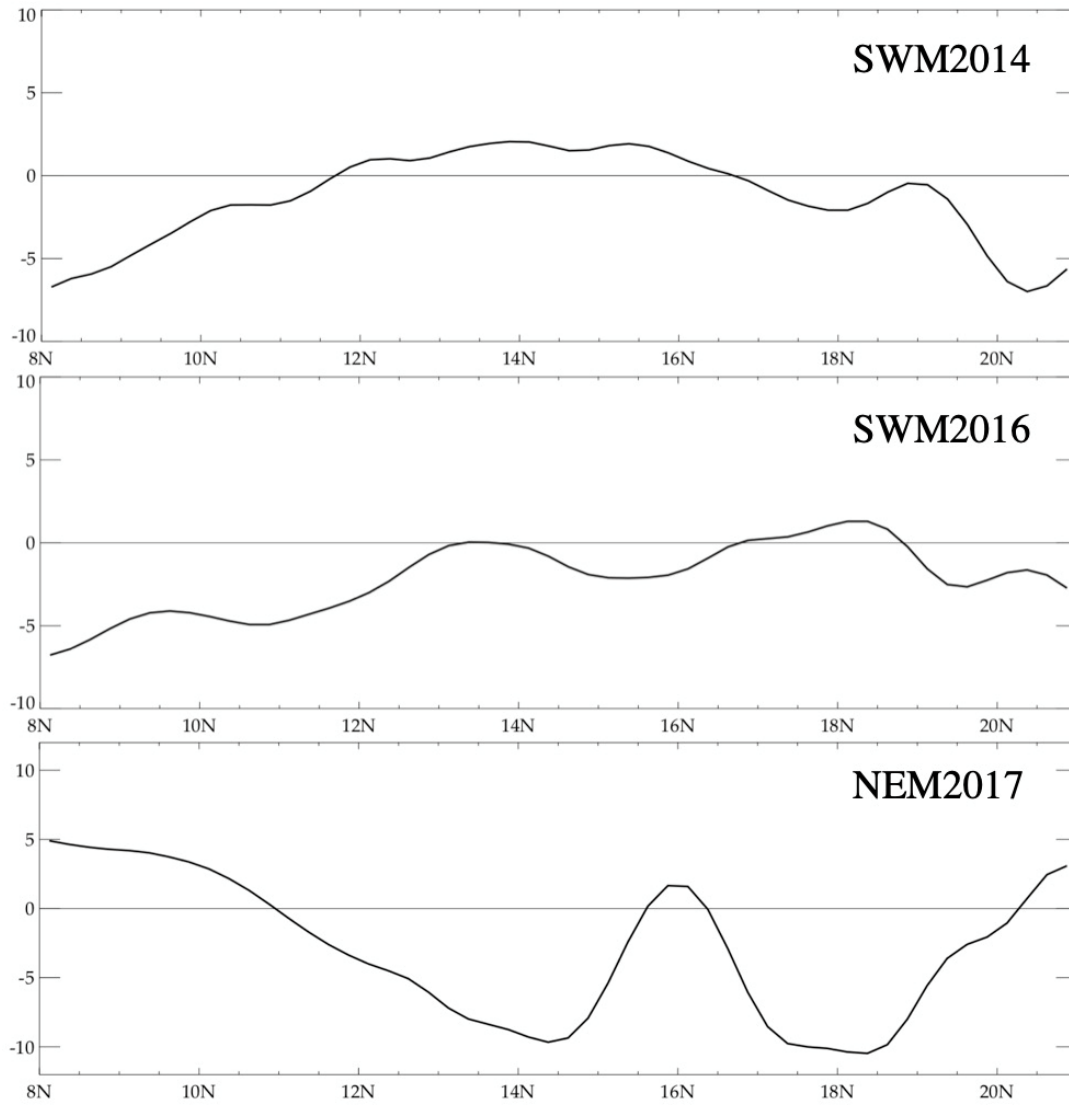


Figure 7. Observed sea level (in cm) along 68°E between 8 and 21°N (i.e. along the observational track) during the SWM of 2014 and 2016 and, the NEM of 2017. Positive sea level indicates downwelling, whereas negative sea level indicates upwelling conditions.

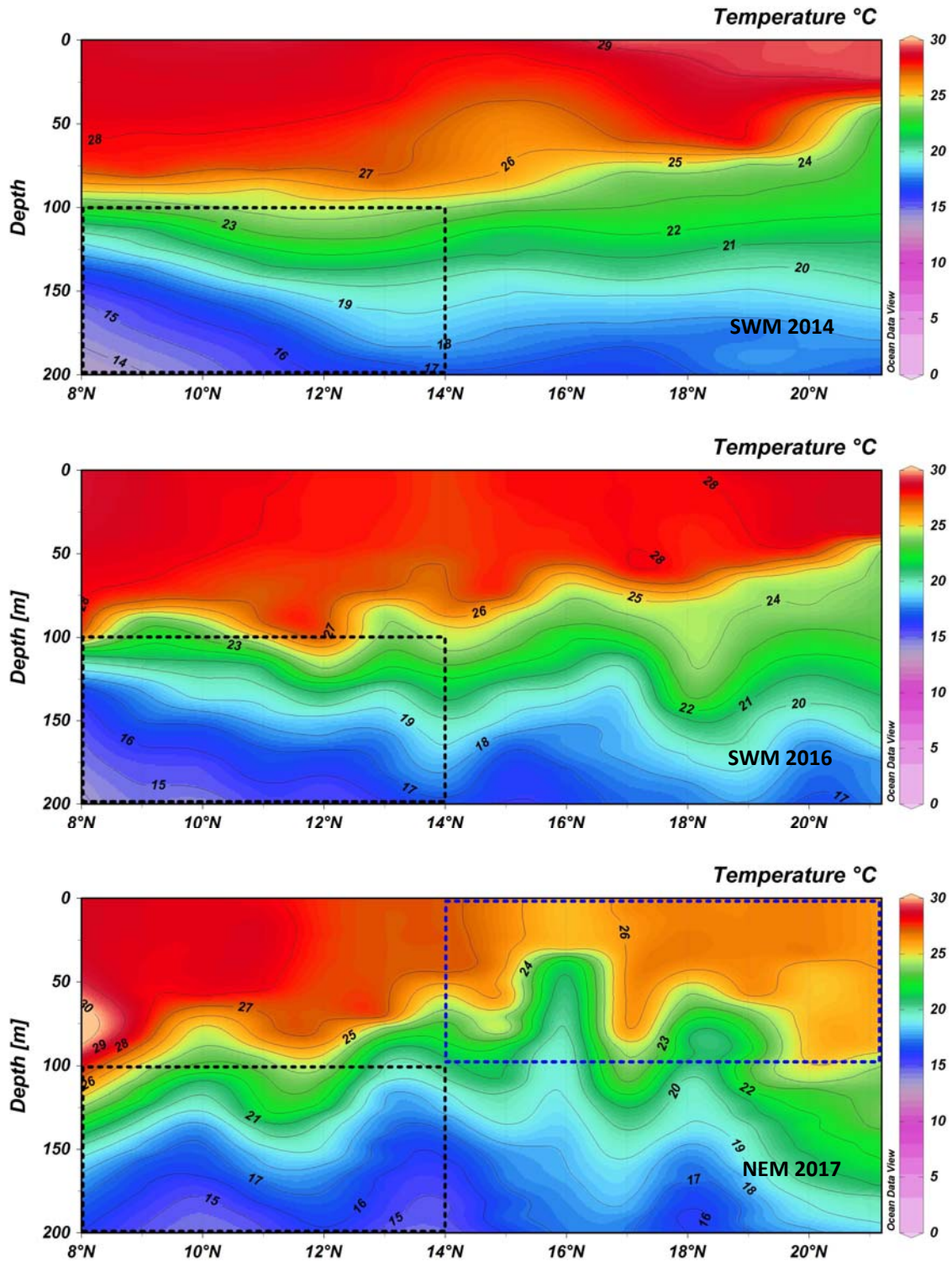
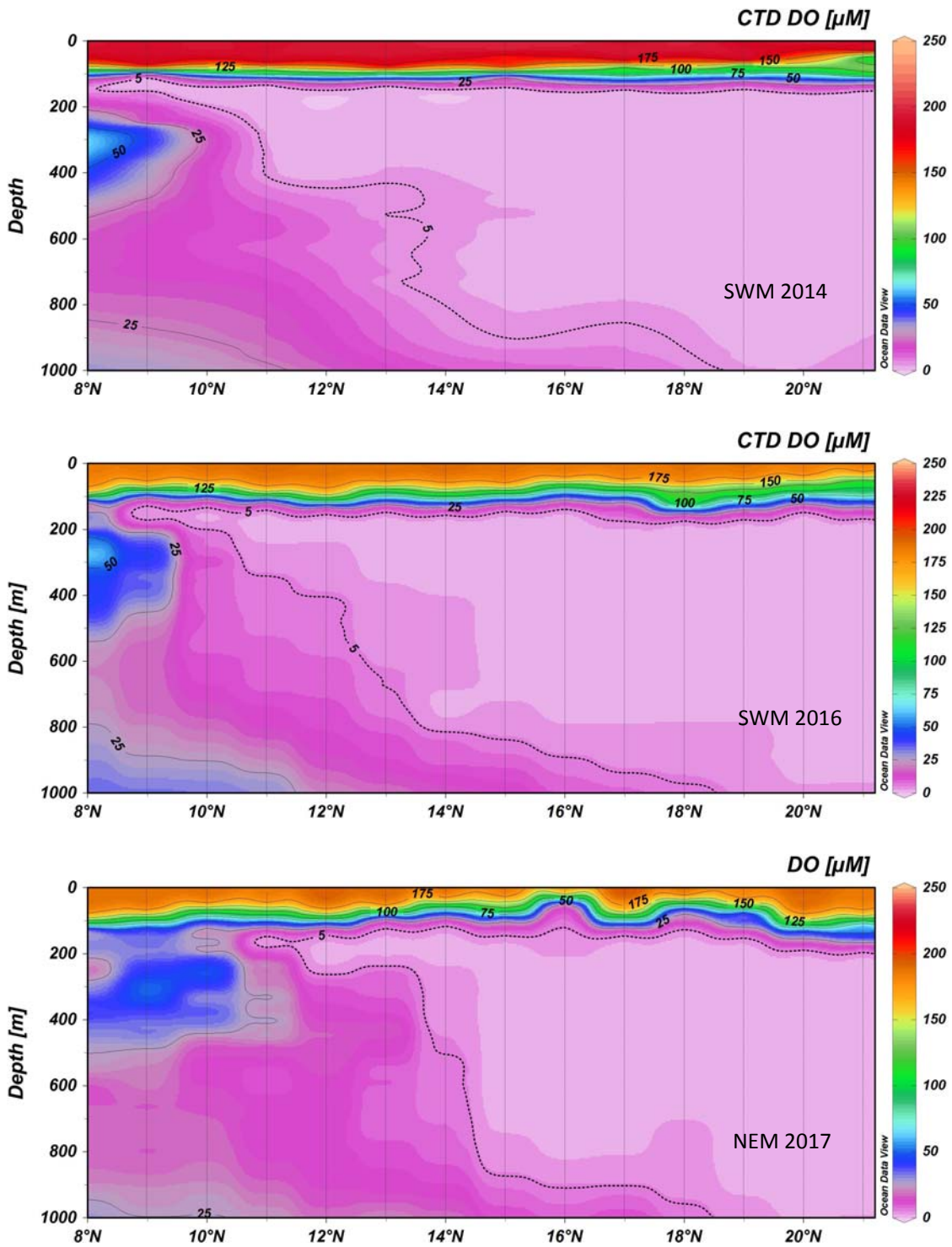


Figure 8. Temperature profiles for the top 200 m during the SWM of 2014 and 2016 and the NEM of 2017. The black dotted boxes show lower temperature isotherms during the SWM of 2016 and NEM of 2017 in comparison to the SWM of 2014 between 100 and 200 m. The blue dotted box shows lower temperature isotherms in the top 100 m indicating winter mixing and also shows the deepening of the isotherms below 100 m.



Supplementary Figure. Variation of CTD dissolved oxygen (at 1 m interval) between 8 and 21°N along 68°E longitude during the SWM of 2014 and 2016, and during the NEM of 2017.